

1 A METHOD FOR IMPROVING THE MEASUREMENT OF LOW-FIELD
2 MAGNETIC SUSCEPTIBILITY ANISOTROPY IN WEAK SAMPLES

3

4 **Authors:**

5 Andrea R. Biedermann, William Lowrie, Ann M. Hirt

6 Institute of Geophysics, ETH Zurich, Sonneggstrasse 5, 8092 Zurich

7

8

9 The final version of this article can be downloaded from the Journal of Applied Geophysics webpage,
10 DOI: [10.1016/j.jappgeo.2012.10.008](https://doi.org/10.1016/j.jappgeo.2012.10.008)

11 **Abstract**

12 Many minerals and rocks have low susceptibilities and magnetic anisotropies on the order of the noise
13 level of the measuring instrument. Anisotropy is often not significant in these samples when using the
14 standard measurement procedure. We propose a method that uses stacking of data to improve the
15 signal-to-noise ratio, thus extending the dynamic range for measurement and allowing for assessment
16 of the data quality. The method makes it possible to obtain consistent directions of the principal axes
17 for samples with an anisotropy on the order of, or even slightly below, the noise level of the
18 instrument. For noisy datasets, the stacking procedure makes it easier to recover correct directions.
19 However, the degree P and shape U of the anisotropy ellipsoid show large variations. Large values of
20 P , in combination with a badly defined U , may indicate noisy data rather than a large anisotropy. The
21 stacking procedure is especially useful for determining the magnetic anisotropy of single crystals that
22 often have a low susceptibility but must be measured with high accuracy.

23

24 **Keywords:** Magnetic susceptibility anisotropy, mineral magnetic fabric, susceptibility bridge, single
25 crystal anisotropy, weak samples

26 **1. Introduction**

27

28 During the formation or deformation of a rock or sediment the mineral grains may experience
29 partial alignment, which causes physical properties to be anisotropic. In this case the magnetic
30 susceptibility can be described mathematically by a second-order symmetric tensor and represented
31 geometrically by an ellipsoid. The principal axes of this ellipsoid, $k_1 \geq k_2 \geq k_3$, have lengths
32 corresponding to the eigenvalues of the tensor. The mean susceptibility is defined as the average of the
33 eigenvalues: $k_{mean} = \frac{1}{3}(k_1 + k_2 + k_3)$.

34 The potential usefulness of the anisotropy of magnetic susceptibility (AMS) as a petrofabric
35 indicator was first indicated by Graham (1954), but was not investigated widely for many years. An
36 early use of AMS was made in the investigation of the deflection of remanent magnetization away

37 from the applied field direction by rock magnetic fabric (Fuller, 1960; 1963). This could result in
38 errors of interpretation in studies of the paleomagnetic field, and might also cause inaccuracies in
39 total-field magnetic anomaly studies. AMS was investigated as a means of correcting for these effects.
40 Many studies of the relationship between AMS and mineral fabric have established the usefulness of
41 AMS as a proxy for current directions in sediments (Hamilton and Rees, 1970), deformation or strain
42 in deformed rocks (Graham, 1966; Kligfield et al., 1981; Hrouda, 1982), and flow directions in
43 igneous rocks (Stacey, 1960). Comprehensive reviews of these applications of AMS have been made
44 by Borradaile and Henry (1997), Borradaile and Jackson (2010) and Tarling and Hrouda (1993).

45 In order to relate AMS to the mineral fabric, it is important to understand which mineral
46 carries the anisotropy. This is not necessarily the mineral with the highest intrinsic susceptibility (such
47 as magnetite or pyrrhotite), which may only be present in trace amounts. Many common rock-forming
48 minerals (such as quartz, feldspars, calcites) have a low susceptibility and/or a weak anisotropy. In
49 addition, mineral groups such as amphiboles or pyroxenes can also have very low susceptibilities,
50 depending on their chemical composition. When AMS is used as an indicator for mineral fabric in
51 rocks whose constituent minerals are made up largely of these phases, it is difficult to extract the
52 useful signal from the measurement noise, even with instruments of high sensitivity.

53 Two methods are commonly used to measure magnetic anisotropy. The first consists of
54 determining the full susceptibility tensor, whereas the second measures the deviatoric susceptibility
55 tensor. The full tensor can be obtained by measuring the susceptibility in specified directions relative
56 to sample coordinates. This static technique can be used with susceptibility bridges, such as the
57 AGICO KLY or the MFK1. The measurement scheme requires the determination of at least 6
58 directional susceptibilities to compute the 6 independent elements of the symmetric (3×3)
59 susceptibility tensor. The AMS ellipsoid is estimated by a least-squares fit to the directional data. If
60 more than the minimum number of measurements are made, the ellipsoid is over-defined and the error
61 of fitting can be determined. For example, with the AGICO instruments the susceptibility is measured
62 in 15 directions, so the data quality and significance of the AMS can be estimated (Jelinek, 1977).
63 Another way to determine the full susceptibility tensor utilizes the high-field slopes of hysteresis loops

64 (Kelso et al., 2002). This method uses 24 different orientations of the sample to the field direction and
65 yields the paramagnetic component of the anisotropy.

66 The second method of determining AMS measures the deviatoric susceptibility tensor. This is
67 generally done by rotating the sample in a magnetic field successively in three mutually orthogonal
68 planes. Such measurements can be made with a spinner magnetometer or with a susceptibility bridge.
69 They can also be made with a torque magnetometer, in which a sample is suspended in an applied
70 field and the torque which the sample experiences due to its anisotropy is measured as a function of
71 applied field in the three orthogonal planes. Used in strong fields this method can be used to separate
72 the fabrics of ferromagnetic (s.l.) and paramagnetic mineral fractions in a rock. In low applied fields
73 the rotational technique forms the basis of anisotropy analysis with spinner magnetometers, such as
74 the AGICO KLY-3S, KLY-4S and MFK1, and the Digico and MiniSpin instruments. The signal of the
75 rotating sample is a sine curve whose frequency is twice that of the rotation. In principle, half a
76 revolution in each of the three planes would be enough to determine the signal. In practice, the signal
77 is measured over a full revolution in the high-field torque magnetometer and is averaged over many
78 cycles in the spinner magnetometers. The absolute tensor can be calculated by measuring the
79 susceptibility in a specific direction and adding this to the deviatoric tensor.

80 According to Jelinek (1996), the deviatoric tensor can be measured with higher precision and
81 better sensitivity than the full tensor. For example, the KLY-4S instrument has a higher sensitivity
82 (2×10^{-8} SI) for anisotropy measurements than for bulk susceptibility (3×10^{-8} SI). Instrument
83 development has led to ever-increasing sensitivity; the MFK1 susceptibility bridges have a sensitivity
84 level of 2×10^{-8} SI at a frequency of 976 Hz and in a field of 400 A/m.

85 In general, if a sample has a high susceptibility and is strongly anisotropic, measurements with
86 any of the above methods are reproducible within small measurement errors. However, for samples
87 with a low susceptibility or a weak anisotropy the noise level of the measurement may be on the order
88 of the anisotropy of the sample. Consequently, subsequent measurements of the same specimen can
89 give strongly different results in terms of the degree, shape and principal directions of the anisotropy
90 ellipsoid.

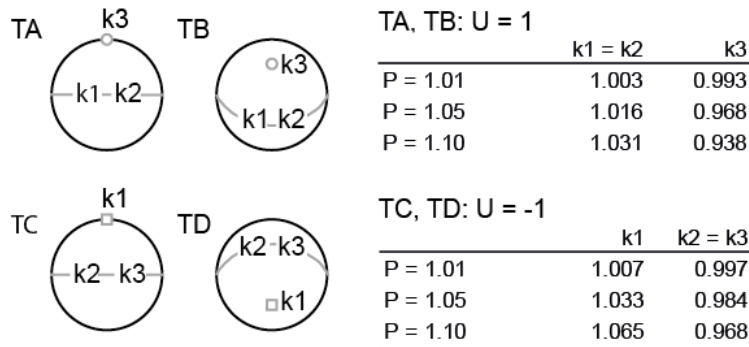
91 Our interest in increasing the resolution of AMS measurements stems from the goal of
92 determining the fundamental anisotropy of single crystals of rock-forming minerals, which is related
93 to the crystallographic axes. This requires measurements that are accurate and precise, because
94 minerals with low iron-content (e.g. tremolite, diopside or feldspars) have bulk susceptibilities that can
95 be weakly paramagnetic or diamagnetic. The anisotropies of these minerals can be difficult to measure
96 reliably.

97 In this report we evaluate a method to extend the instrumental resolution and obtain significant
98 results for samples and crystals with very weak anisotropies. The measurements for this study were
99 made with the MFK1-FA in the static operational mode. Further comparison is made with the same
100 instrument in spinning mode. With the data from the static mode, we define a measure for (1)
101 determining if the sample is significantly anisotropic, and (2) evaluating how well the degree, shape
102 and principal directions are defined by the AMS data. In order to understand the variation of the
103 susceptibility parameters for weak samples, model calculations are performed for synthetic data with
104 different degrees and shapes of anisotropy. This part of the study leads to a way of assessing the
105 quality of AMS measurements. Finally, the method is applied to real samples with a range of bulk
106 susceptibilities and anisotropies.

107 **2. Synthetic data**

108

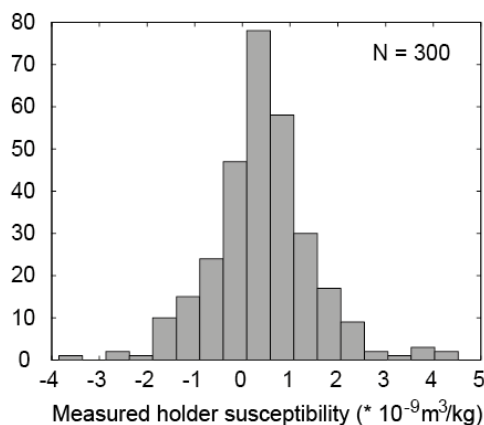
109 Four AMS tensors have been investigated by analysis of synthetic data (Fig. 1): two
110 rotationally *oblate* ellipsoids, with either horizontal or tilted k_3 (minimum) axes (TA and TB,
111 respectively) and two rotationally *prolate* ellipsoids with horizontal or tilted k_1 (maximum) axes (TC
112 and TD, respectively). For each of these tensors, anisotropy degrees of $P = 1.01, 1.05$ and 1.10 were
113 analyzed. These synthetic datasets correspond to the typical anisotropies for the amphibole and
114 clinopyroxene mineral groups. The directional values for the susceptibility that are usually measured
115 were computed for each of these cases.



116

117 Figure 1: Directions of principal axes of the susceptibility tensors from which the synthetic data were
 118 calculated.

119 In weakly magnetic samples the signal of the sample holder may be similar to, or greater than,
 120 that of the sample and must be compensated. In order to obtain an idea of the noise distribution of the
 121 MFK1 instrument, the empty holder was measured 300 times and the standard correction for the
 122 holder made each time. As expected, the measurements cluster about a value of zero. Figure 2 shows
 123 that we can assume a normal distribution for the noise. The noise measurements were compared to
 124 typical mean susceptibilities for different samples of amphiboles, pyroxenes or feldspars. This
 125 comparison shows that the instrumental noise levels is commonly up to 20% of the mean
 126 susceptibility, while for certain feldspar crystals they can amount to as much as 300% of the mean
 127 susceptibility.



128

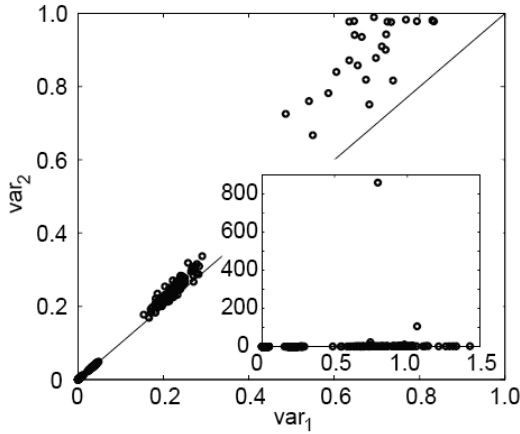
129 Figure 2: Susceptibility values of 300 holder measurements after correction for the holder
 130 susceptibility. The data correspond to the noise distribution of the MFK1 and follow a normal
 131 distribution.

132 In order to simulate noisy data from our synthetic tensors, we first computed directional
133 susceptibilities for the 15 positions that are routinely measured. Noise was simulated by selecting
134 random numbers from a normal distribution with zero mean-value whose standard deviation was
135 successively set equal to different values between 1% and 100% of the mean susceptibility of the
136 synthetic sample. Defining noise as a percentage of the mean susceptibility has the advantage that our
137 results are valid for arbitrary mean susceptibilities. The computed noise was added to the directional
138 data. Ten datasets were generated, each consisting of 3, 5, 7 or 10 values for each of the 15
139 measurement positions. This was repeated for every combination of susceptibility tensor, AMS
140 degree, and noise level. In addition, 20 isotropic datasets were generated with the same noise
141 distribution as in the anisotropic data. The repeated values at each measurement position were then
142 averaged. In this way, statistical noise is cancelled whereas the signal due to the magnetic
143 susceptibility anisotropy is enhanced. For comparison, individual AMS ellipsoids were also
144 determined from all of the first, second, ... and fifteenth values at each position.

145 The AMS ellipsoid was computed by performing a least-squares-fit for each averaged or
146 individual dataset. From this, one obtains the magnitudes and directions of the principal
147 susceptibilities. The shape and degree of the anisotropy ellipsoid for each of the individual datasets
148 can then be compared to the same anisotropy parameters of the averaged dataset. The anisotropy
149 ellipsoid is characterized from the AMS data by its degree, $P = k_1/k_3$ (Nagata, 1961) and by its
150 shape $U = (2k_2 - k_1 - k_3)/(k_1 - k_3)$ (Jelinek, 1981). P is equal to 1 in the isotropic case and
151 increases with increasing anisotropy. The parameter U can have values between -1, for rotationally
152 *prolate* ellipsoids, and +1, for rotationally *oblate* ellipsoids.

153 Data quality and significance of the anisotropy are evaluated by comparing the deviation of
154 the ellipsoid from a sphere to the amount of noise. Two estimates for a noise parameter were
155 investigated for the stacked datasets: $var_1 = (\sum_{i=1}^{15} \Delta a_i^2) / (\sum_{i=1}^{15} \bar{a}_i^2)$ and $var_2 = \sum_{i=1}^{15} (\Delta a_i / \bar{a}_i)^2$
156 where $\Delta a_i^2 = \frac{1}{10} \sum_{j=1}^{10} (a_{ij} - \bar{a}_i)^2$, $\bar{a}_i = \frac{1}{10} \sum_{j=1}^{10} a_{ij}$ and a_{ij} is the j^{th} measurement in the i^{th} position.
157 The parameters var_1 and var_2 have the same values for small noise levels. For most datasets, the two
158 parameters vary proportionally to each other (Fig. 3). However, if the noise is comparable to the signal

159 and the mean value in one direction is close to zero, var_2 will increase dramatically, whereas var_1 will
 160 remain stable (Fig. 3, inset). For this reason only var_1 will be considered further.



161
 162 Figure 3: A comparison of var_1 and var_2 of all anisotropic synthetic datasets shows that var_2 increases
 163 strongly for certain datasets, whereas the variation in var_1 is smaller. Inset: Effect of near-zero mean
 164 value on parameter var_2 .

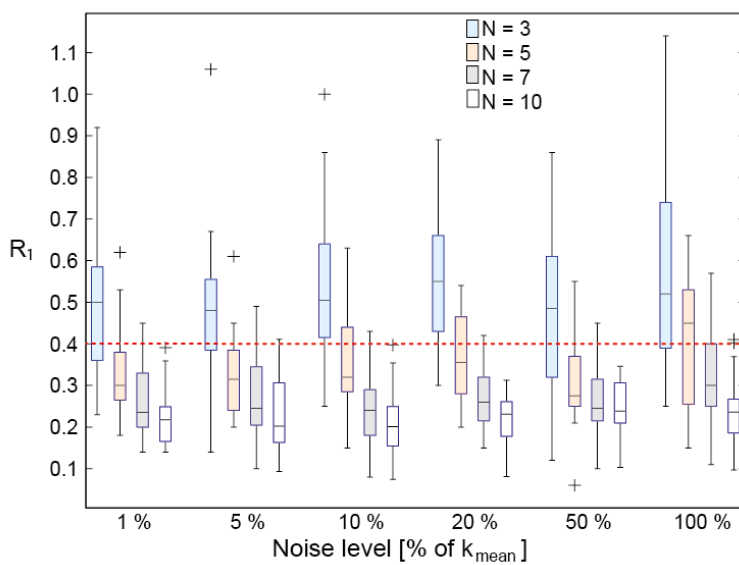
165
 166 The deviation of the ellipsoid from a sphere, dev , is described by Jelinek (1977) as
 167 $dev = (k_1^2 + k_2^2 + k_3^2 - 3k_{mean}^2) / ((N-1)k_{mean}^2)$, where $N = 6$ is the number of independent elements in the
 168 susceptibility tensor and k_{mean} is the mean susceptibility.

169 The parameter that we have used to assess the significance of the AMS is $R_1 = \sqrt{dev/var_1}$.
 170 The larger this parameter, the better defined is the anisotropy compared to the noise level. The largest
 171 value obtained with isotropic data is used to define the lower threshold for assessing whether or not
 172 the sample is anisotropic. All samples that are below this threshold are considered not to exhibit a
 173 significant anisotropy.

174 2.1 Results for isotropic data

175
 176 Analysis of isotropic synthetic datasets allows us to estimate a threshold of significance for the
 177 anisotropy determined from a given dataset – synthetic or measured. Synthetic datasets were computed
 178 for isotropic samples assuming the different noise levels described in the previous section. A set of 20

179 datasets was generated for each noise level. The parameter R_1 depends on the number of values that
 180 are averaged; it is generally smaller and shows less variation when the number of datasets that are
 181 averaged increases (Fig. 4). Basing the stacking of data on 10 (measured or synthetic) values gives
 182 slightly more consistent results than using $N = 7$ data, and significantly lower noise parameters than
 183 using $N = 3$ or 5. For a stack of ten isotropic datasets, the ratio R_1 was found to be less than 0.4,
 184 independently of the noise level. Thus, AMS data for samples with a ratio of less than 0.4 should be
 185 rejected, as their anisotropy is not significant.



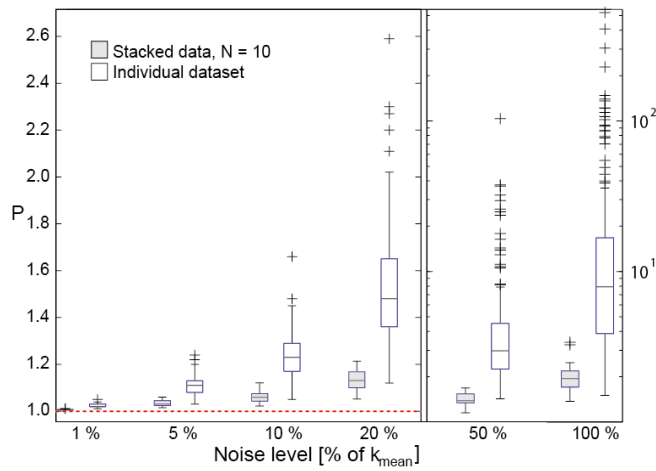
186

187 Figure 4: Results for isotropic synthetic data with different noise levels and sizes of datasets ($N = 3, 5,$
 188 7 and 10 repeated measurements per position). R_1 decreases with increasing N , independently of
 189 the noise level. The line represents the median of the data, the box extends from the 25th to the 75th
 190 percentile and the whiskers can be interpreted as the 1st and 99th percentiles. Crosses represent
 191 values considered as outliers. Dotted line shows R_1 -value used to distinguish if the sample is
 192 anisotropic.

193

194 The degree of anisotropy, P , should equal 1.00, because the input data are isotropic. However,
 195 P is seen to increase strongly with increasing noise level. This increase is less pronounced in the
 196 stacked data than for the individual datasets (Fig. 5). Therefore, a large P does not necessarily
 197 correspond to strong anisotropy, but could merely be an indication of poor data quality. This is
 198 especially the case when a large P is associated with a large variation in the repeated measurements.
 199 Principal directions are random in this situation, which indicates that no preferential direction is

200 introduced by the data processing. The only parameter that remains well-defined, independent of noise
 201 level, is the mean susceptibility (Tab. 1).



202
 203 Figure 5: The anisotropy degree P for isotropic synthetic data. P should equal 1, however it increases
 204 with increasing noise level. This effect is less pronounced for the stacked than for the individual
 205 datasets. Note the change of vertical scale: on the left the scale is linear, on the right it is logarithmic.

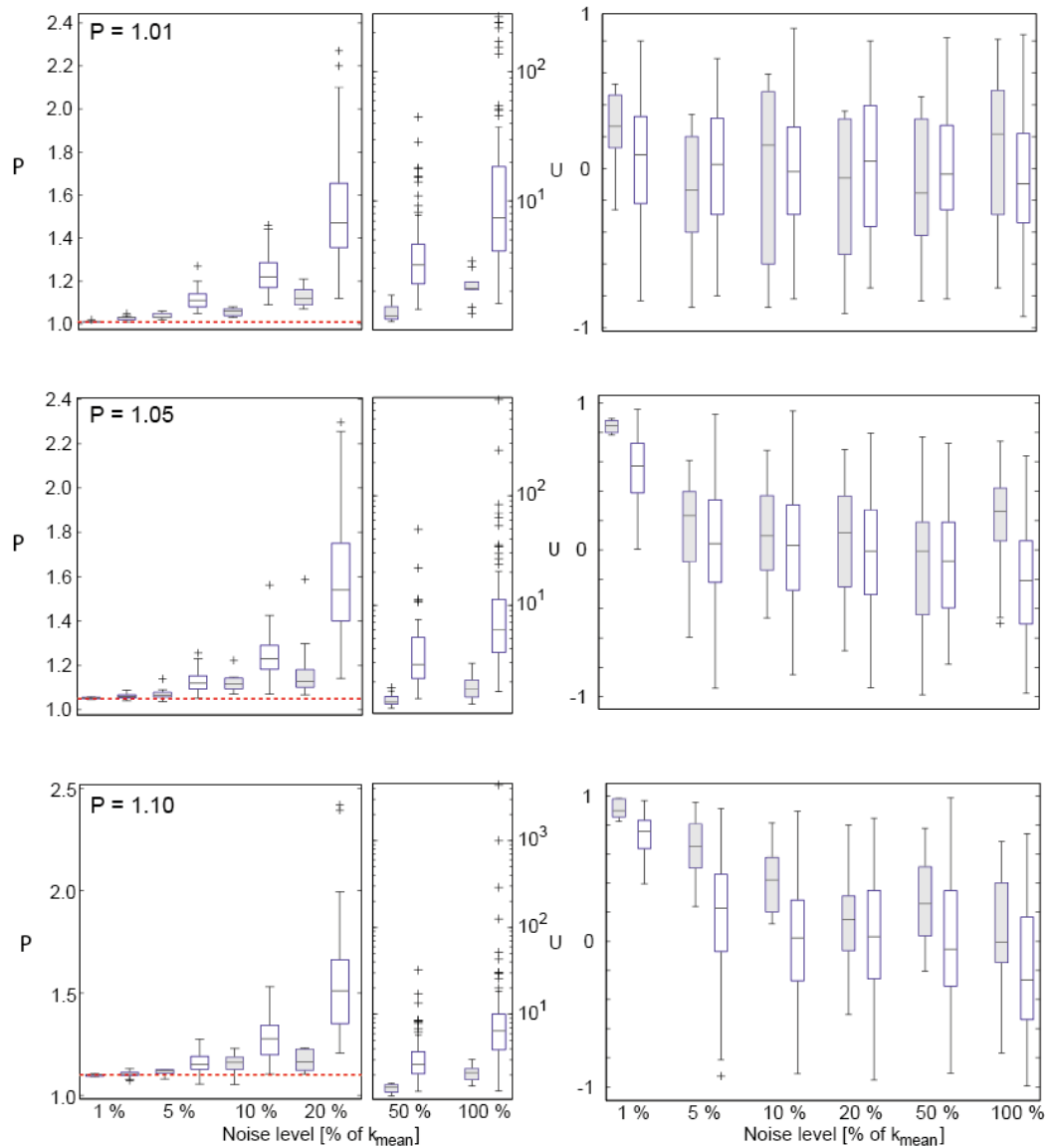
206

207 2.2 Results for anisotropic data

208

209 Results for the synthetic anisotropic data are summarized in Table 2 (electronic supplementary
 210 material). Again, we generated data with $P = 1.01, 1.05$ and 1.10 and noise levels of 1% to 100% of
 211 the mean susceptibility for the four tensors. The isotropic data show that best results are achieved with
 212 stacking 10 measurements at each position. Therefore, $N = 10$ was used for further analysis. Tensor
 213 TA (Fig. 6 and 7) illustrates how ellipsoid shape and axial directions vary with the degree of
 214 anisotropy and the noise level. As with the isotropic data, P increases when the noise increases.
 215 Furthermore, the variation in U increases with the amount of noise. For the individual measurements,
 216 the shape already varies from oblate to prolate and is not reliable when $P = 1.10$ and the noise level is
 217 5%. Even for 1% noise, the U values indicate the correct region – oblate or prolate – but show large
 218 variations between individual datasets. The increase of the AMS degree P to unrealistically high
 219 values is much more pronounced in the individual datasets than for the stacked data. The directions of
 220 the stacked datasets agree reasonably well with the true directions, even when the noise level is

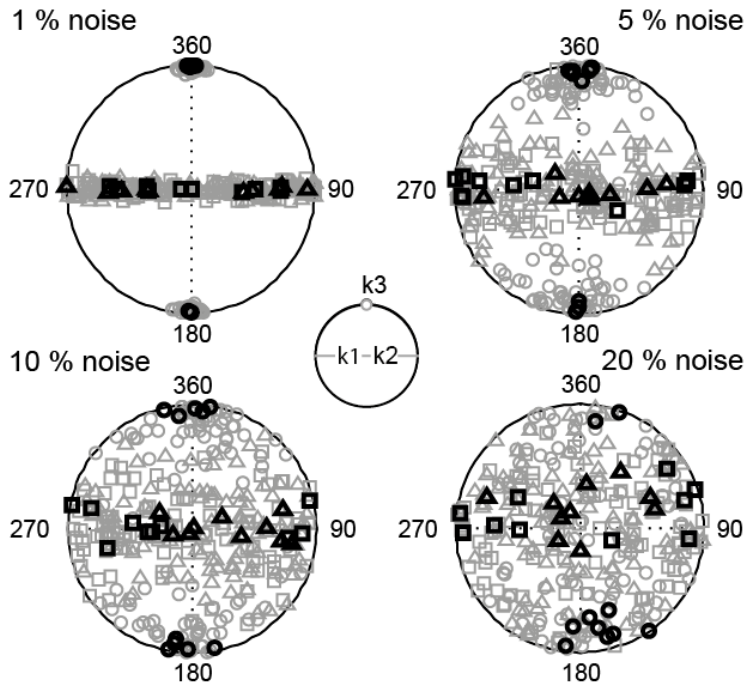
221 slightly larger than the degree of AMS. This is even the case when the directional data of the
 222 individual measurements appear to be nearly randomly distributed and both U and P show large
 223 variations.



224

225 Figure 6: P and U computed from synthetic datasets with oblate shape and (a) 1%, (b) 5% and (c) 10%
 226 anisotropy. The green line shows the expected anisotropy degree P for these cases. The shape
 227 parameter U should be equal to one.

228



229

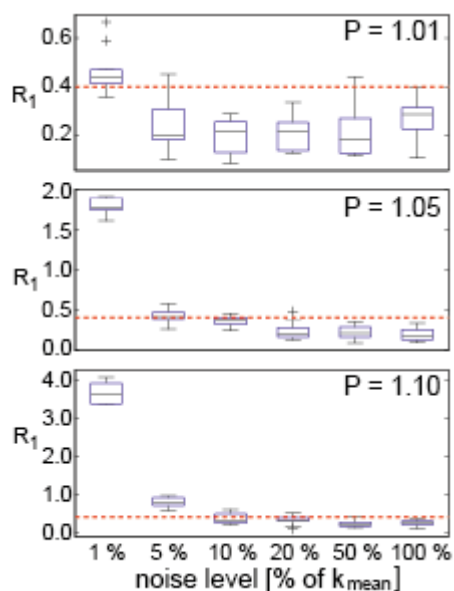
230 Figure 7: Principal susceptibility directions for an oblate ellipsoid with 10% AMS and different noise
 231 levels. The expected solution is a cluster of k_3 axes at 360° and a girdle of $k_1 = k_2$ axes in a plane
 232 perpendicular to k_3 , as suggested in the small central plot. Minimum directions are grouped around
 233 the true direction even when the noise level is 20% and thus twice the anisotropy. In these equal-
 234 area, lower hemisphere stereoplots squares, triangles and circles refer to the maximum,
 235 intermediate and minimum principal susceptibility, respectively. Grey symbols represent individual
 236 data and dark symbols represent the stacked values in this and subsequent figures.

237

238 The usefulness of R_1 as an indicator of data quality is illustrated in Figure 8. For example, for
 239 an anisotropy degree of 1.10 and noise of 1%, R_1 is nearly an order of magnitude larger than the
 240 threshold of 0.4, and the principal directions, shape and degree of the AMS ellipsoid coincide with the
 241 input parameters. However, if $P = 1.10$ and the noise is 5%, the values for R_1 are between 0.5 and 1,
 242 only slightly above the 0.4 limit. In this case, the directions and the degree of the ellipsoid can be well
 243 resolved, but the shape shows a large variation between the individual data stacks. If the anisotropy
 244 degree is $P = 1.10$ and the noise is 10%, the directions of the ellipsoid principal axes are reasonably
 245 well resolved, but the data for the AMS shape are no longer reliable and the AMS degree is too large.

246 In summary, the anisotropy ellipsoid can be recovered well from the stacked values, provided
 247 the noise level of the measurements does not exceed the degree of anisotropy of the sample. The
 248 directions are defined better than the degree of anisotropy and the ellipsoid shapes. When the noise

249 level is less than the anisotropy, the anisotropy degree and shape are well defined, but when the noise
 250 level is larger than the AMS, P increases to unrealistically high values and U covers the whole range
 251 from prolate to oblate ellipsoids. The known input values are recovered better by the stacked data than
 252 by the individual datasets. For weak samples, where the anisotropy is on the order of the noise level,
 253 stacking makes it possible to obtain reliable data that otherwise could not be derived. P and especially
 254 U may not be recovered when the anisotropy is on the order of – or smaller than – the noise level.
 255 However, even then it is possible to determine the principal directions. For example, directional data
 256 of the individual datasets appear to be random when the noise level is above the degree of anisotropy,
 257 yet the stacked datasets still cluster along the true directions, as shown in Figure 7.



258
 259 Figure 8: Ratio R_1 for the synthetic oblate amphibole datasets shown in Figure 3. Where R_1 is below
 260 0.4, the AMS data are not significant. Dotted line shows $R_1 = 0.4$.

261 3. Rock samples

262 3.1 Method

263
 264 Low-field AMS was analyzed for a collection of single crystals of amphiboles and pyroxenes.
 265 Samples were measured on an AGICO MFK1-FA Kappabridge in a field of 200 A/m. Each position
 266 was recorded ten times and weak samples were remeasured in a 500 A/m field to enhance the
 267 signal/noise ratio. As for the synthetic data, individual as well as stacked datasets were analyzed.

268 Sample and background were remeasured in the same position 10 times and averaged to obtain the
269 stacked dataset. It is assumed that these repeated measurements give independent estimates of the
270 susceptibility value in each sample direction. Repeated measurements of the same position were
271 plotted against time to check for instrumental drift, which was negligible in all samples. Samples were
272 chosen so as to cover a wide range of susceptibilities within the same mineral group. If the AMS
273 correlates with the crystallographic structure of the mineral, the ellipsoid shape and its principal
274 directions should be comparable for a range of chemical compositions.

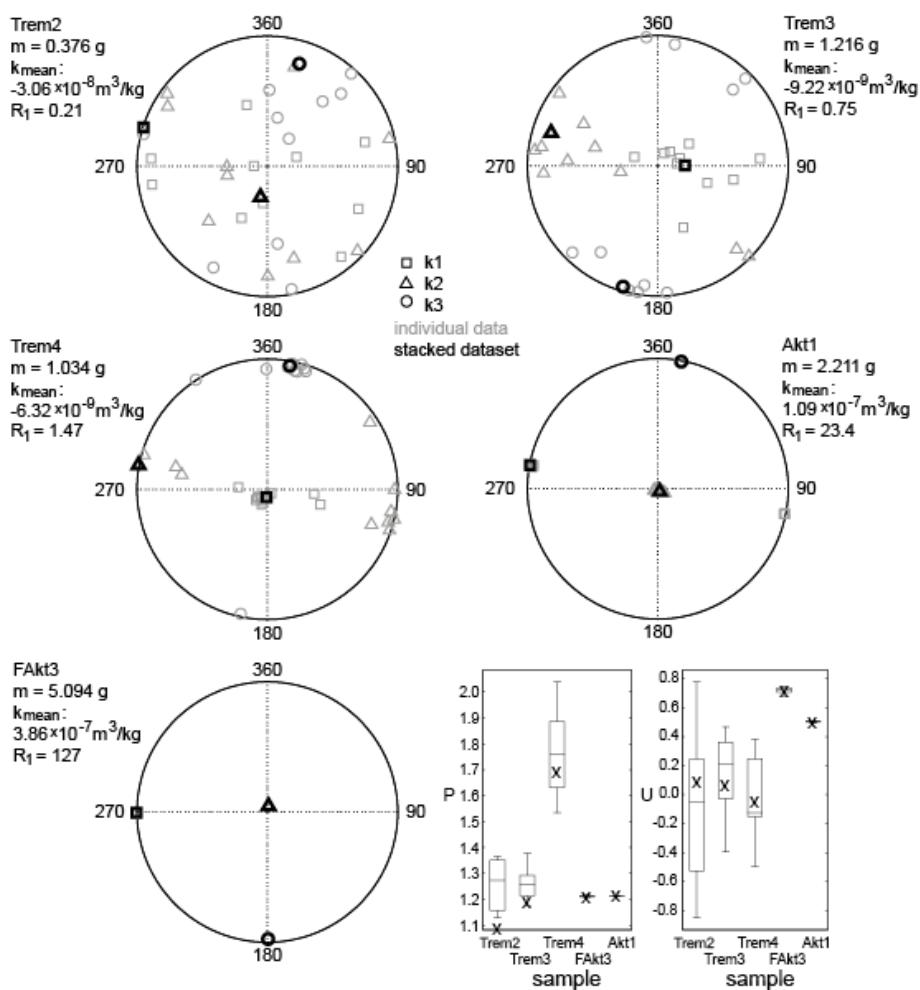
275 **3.2 Results**

276

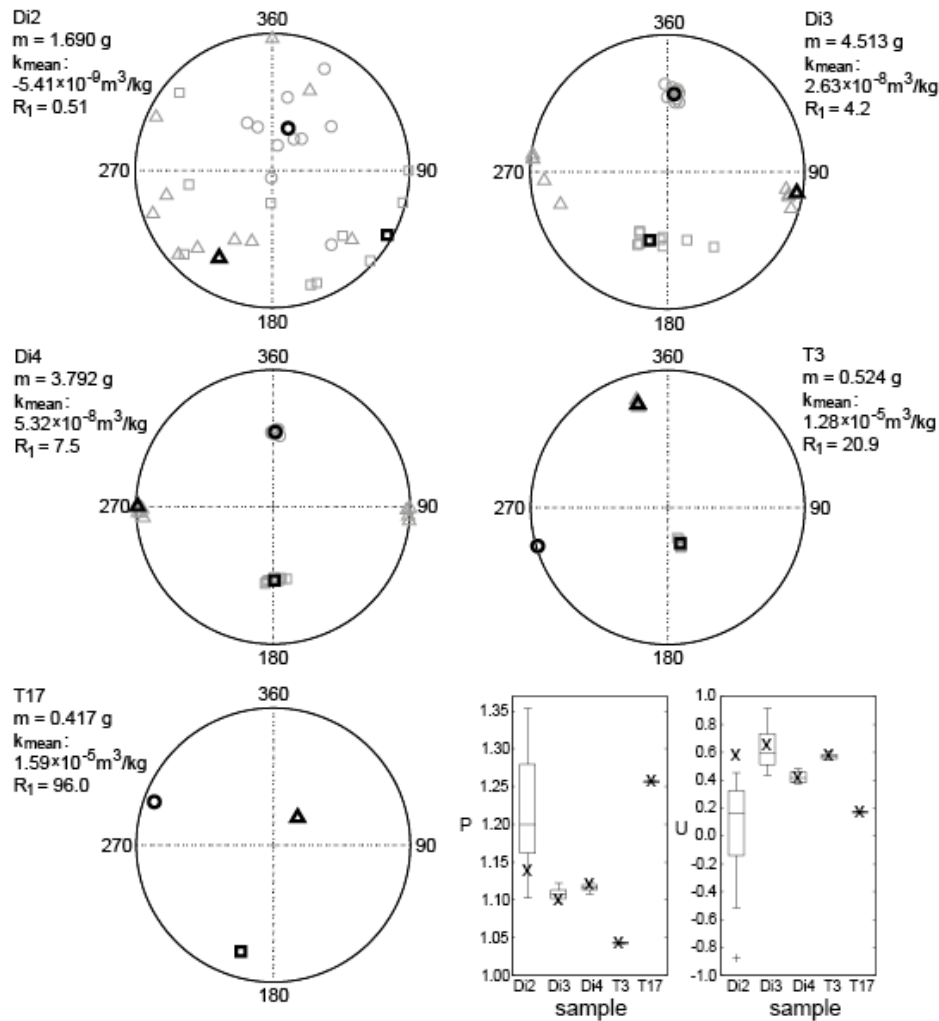
277 For samples with strong susceptibility and/or a large degree of anisotropy, the noise is very
278 small compared to the signal and stacking brings no advantage, as can be seen for the actinolites
279 (samples Akt1 and FAkt3, Fig. 9) and augites (T3 and T17, Fig. 10). The individual measurements
280 coincide with each other. The agreement of the directions is, however, more consistent than the
281 agreement of the degree and shape of the anisotropy ellipsoid.

282 In the case of samples that have a low susceptibility, or those with a weak anisotropy, the
283 noise is comparable to the signal (e.g. Trem2, Trem3 and Di2). In this case, stacking substantially
284 improves the signal quality. The noise parameter for Trem2 is below the threshold of 0.4, and thus the
285 anisotropy of Trem2 is considered not to be significant. Sample Di2 has a value of R_I slightly above
286 the threshold; whereas the individual measurements show a large variation, the minimum direction of
287 the stacked dataset is very close to that expected from results in the other diopsides. Compared to the
288 other diopsides the discrepancy is larger for the directions of the maximum and intermediate principal
289 axes, because diopside possesses an oblate-shaped AMS ellipsoid. The anisotropy parameters U and P
290 show large variations for the individual datasets of Di2, but the stacked values are similar to the
291 expected values as determined from Di3 and Di4. Similarly, Trem3 displays a large variation in the
292 individual datasets, but the stacked values agree well with the better-defined AMS parameters of
293 samples with higher susceptibility or stronger degree of anisotropy. Trem2, Trem3, Trem4 and Di2
294 display negative susceptibilities in all directions and thus all principal susceptibilities are negative. For
295 these samples, AMS parameters were defined in terms of the absolute values of the principal

296 susceptibilities. This convention causes problems in samples that have positive susceptibilities in some
 297 directions and negative in others, e.g. when $k_1 > 0$ and $k_3 < 0$. On the other hand, it allows direct
 298 comparison with high-field torque data, as the torque signal is indifferent to whether the magnetization
 299 is parallel (in the paramagnetic case) or antiparallel (in the diamagnetic case) to the magnetic field, but
 300 depends on the angle between the easy magnetization axis and the magnetic field direction. The most
 301 negative susceptibility, i.e. highest absolute value, in a diamagnetic sample corresponds to the easy
 302 axis of magnetization.



303
 304 Figure 9: Principal directions, shape and degree of AMS for amphiboles with different data quality.
 305 The larger R_1 , the better defined are the data. Directions are close to the expected values even when
 306 R_1 is slightly less than 0.4. Good data can also be obtained with individual datasets for $R_1 > 10$. For
 307 Trem4, directional data are consistent within reasonable errors, whereas there is a large spread of
 308 both P and U . In this case, stacking leads to a significant improvement in the results. For Trem3, this
 309 also applies to the directional results.



310

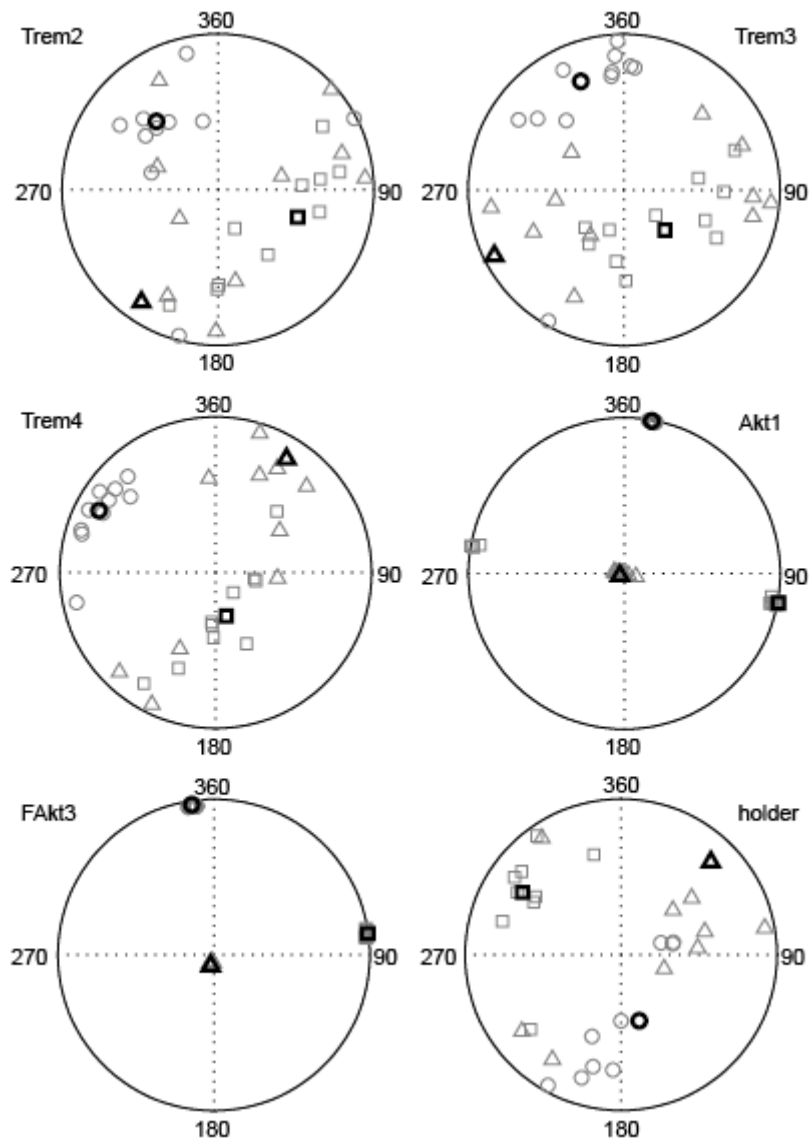
311 Figure 10: AMS results for a selection of clinopyroxenes. Augites T3 and T17 show different directions
 312 than diopsides Di2, Di3 and Di4 because the low-field AMS of the augites is dominated by magnetite
 313 inclusions.

314

315 Diamagnetic and paramagnetic contributions to the AMS are related to atomic positions in the
 316 silicate lattice, thus it is reasonable to assume that all diopsides or all tremolites, respectively, exhibit a
 317 similar AMS ellipsoid. However, this is not true for very strong samples, like T3 and T17, whose
 318 AMS is dominated by the signal of ferromagnetic inclusions. For R_1 between 1 and 10 (Trem3, Di3,
 319 Di4), a clustering of directions already appears in the individual datasets; the larger R_1 , the better the
 320 grouping of directions. In these cases, stacking significantly improves the estimates for anisotropy
 321 degree and shape, whereas the improvement in the directional data is smaller. If R_1 is larger than 10,
 322 stacking is not essential, but it enables an assessment of the data quality.

323 Directions of individual measurements can show a large variation, but when measuring several
324 samples of the same mineral, the stacked directions coincide reasonably well. As is the case for the
325 synthetic data, it appears that for the minerals, as for the synthetic data, the data quality is poor (or the
326 anisotropy not significant) if the factor R_1 is less than 0.4.

327 It is of interest to compare results obtained with the MFK1 instrument in both the static and
328 spinning modes of measurement. A summary of the spinning mode data is shown in Table 3
329 (electronic supplementary material). Figure 11 shows AMS of the same samples as in Figure 9, but
330 measured in the spinning specimen mode. For comparison, the spinned measurements were repeated
331 ten times. The directions of the weak samples (Trem2, Trem3 and Trem4) show a large scatter and
332 appear to be influenced more strongly by the holder signal – even though this is subtracted – than by
333 the anisotropy of the crystal itself. A superposition of signals due to the crystal anisotropy and
334 remaining holder signal is measured, the holder having a positive susceptibility and the crystals a
335 negative susceptibility. Thus, the remaining holder signal is effectively subtracted, which explains
336 why k_1 of the holder relates to k_3 in the tremolite samples. For the stronger samples Akt1 and FAkt3
337 the results are consistent and agree with those from the static mode. The scatter is larger for repeated
338 measurements in the spinning mode. According to F-values and confidence angles that are computed
339 when measuring in the spinning mode, AMS is not significant for Trem2, Trem3 or Trem4 at the 95%
340 level of significance. However, the static measurements show a good grouping about the correct mean
341 direction for Trem4 and, to a lesser extent, Trem3. Only the R_1 value of Trem2 indicates that its AMS
342 is not significant. Thus, a significant improvement with respect to the spinning mode can be achieved
343 by stacking AMS data measured in the static mode.



344

345 Figure 11: AMS results for the same samples as in Figure 9, measured in the spinning specimen mode
 346 of the MFK1. The results of the weak samples (Trem2, Trem3 and Trem4) are strongly influenced by
 347 the anisotropic signal of the holder. Results for the stronger samples (Akt1 and FAkt3) are similar to
 348 those determined in the static mode, but show a larger variation in directions.

349 4. Discussion and conclusions

350

351 There is a strong interest in using AMS to define preferential grain orientation in rocks or
 352 sediments with weak mineral fabrics. These may represent flow directions in the case of lavas or river
 353 deposits, or strain fabrics in the case of deformed rocks. Especially for weak samples it may be the
 354 case that a large spread in individual directions reflects the influence of noise rather than a true
 355 variation in directions. This would explain why Kligfield et al. (1981), in a study of AMS in deformed

356 Permian redbeds, found that, although the anisotropies of redbed specimens displayed a high scatter,
357 the average AMS ellipsoid correlated with the strain ellipsoid.

358 Hrouda (1986; 2004) observed that quartzite, whose bulk susceptibility is close to zero,
359 displays an unrealistically high degree of AMS. He proposed that AMS parameters obtained from
360 samples with bulk susceptibilities between -5×10^{-6} and $+5 \times 10^{-6}$ (SI) should not be used to infer
361 mineral fabric. For low-susceptibility samples, noise contributes significantly more to the
362 measurement than for those with high susceptibility, which probably explains these earlier
363 observations. We have shown that a high noise level causes a large increase in the calculated
364 anisotropy degree. This effect can be reduced by stacking, which yields reliable data for samples with
365 low mean susceptibility.

366 The AGICO susceptibility bridges are highly sensitive, but like any instrument they have a
367 detection limit. The signal generated by the anisotropy of many rocks or minerals may be comparable
368 to instrumental drift (Gee *et al.*, 2008). For this reason, a linear trend is removed from the values
369 measured on AGICO's MFK1 Kappabridge. However, drift is not necessarily linear, and its variability
370 may be an additional source of error. Measuring the deviatoric susceptibility often leads to better
371 precision and higher sensitivity (Jelinek, 1996). However, the present study has shown that, although
372 the stacking of static measurements requires considerably more time to acquire data, it is more
373 effective in determining directional data for very weakly anisotropic samples than the spinning mode
374 of measurement. Magnitudes of principal susceptibilities are more sensitive to measurement noise;
375 however, stacking also improves the definition of the degree of anisotropy and the shape of the AMS
376 ellipsoid. At the same time, stacking allows an assessment of the data quality by means of a simple
377 ratio, and allows definition of a measure of the significance of the AMS. The anisotropy degree P is
378 generally smaller and shows less variation for stacked data. Since P not only increases as a function of
379 anisotropy, but also with increasing noise, this indicates that the signal-to-noise ratio has been
380 enhanced.

381 In particular we have shown for weak samples, for which no reasonable results would be
382 obtained with the standard measurement procedure, that the stacking procedure makes it possible to

383 obtain reasonable results. Therefore, when very exact measurements are needed, as for example to
384 determine the magnetic anisotropy of single crystals, the method of stacking repeated static
385 measurements is recommended.

386 **Acknowledgements**

387 A. Stucki (siber+siber AG, Zurich), S.A. Bosshard and P. Brack (ETH Zurich) are thanked for
388 providing samples. We thank Bernard Henry for his constructive review. This study was funded by the
389 Swiss National Science Foundation (SNF) under project 129806.

390 **References**

- 391 Borradaile, G.J., Henry, B., 1997. Tectonic applications of magnetic susceptibility and its anisotropy.
392 Earth-Sci. Rev. 42, 49-93.
- 393 Borradaile, G.J., Jackson, M., 2010. Structural geology, petrofabrics and magnetic fabrics (AMS,
394 AARM, AIRM). J. Struct. Geol. 32, 1519-1551.
- 395 Fuller, M.D., 1960. Anisotropy of susceptibility and the natural remanent magnetization of some
396 Welsh slates. Nature 186, 790-792.
- 397 Fuller, M.D., 1963. Magnetic anisotropy and paleomagnetism. J. Geophys. Res. 68, 293-309.
- 398 Gee, J.S., Tauxe, L., Constable, C., 2008. AMSSpin: A LabVIEW program for measuring the
399 anisotropy of magnetic susceptibility with the Kappabridge KLY-4S. Geochem. Geophys.
400 Geosyst. 9, Q08Y02.
- 401 Graham, J.W., 1954. Magnetic anisotropy: an unexploited petrofabric element. Bull. Geol. Soc. Amer.
402 65, 1257.
- 403 Graham, J. W., 1966. Significance of magnetic anisotropy in Appalachian sedimentary rocks, in:
404 Steinhart, J.S., Smith T.J. (Eds.) *The Earth Beneath the Continents, Geophysical Monograph*
405 *10*. American Geophysical Union, Washington, pp. 627-648.
- 406 Hamilton, N., Rees, A.I., 1970. The use of magnetic fabric in palaeocurrent estimation, in: Runcorn,
407 S.K. (Ed.), *Palaeogeophysics*, pp. 445-464.
- 408 Hrouda, F., 1982. Magnetic anisotropy of rocks and its application in geology and geophysics.
409 Geophys. Surv. 5, 37-82.
- 410 Hrouda, F., 1986. The effect of quartz on the magnetic anisotropy of quartzite. Stud. Geoph. Geod. 30,
411 39-45.
- 412 Hrouda, F., 2004. Problems in interpreting AMS parameters in diamagnetic rocks, in: Martín-
413 Hernández, F., Lüneburg, C.M., Aubourg, C., Jackson, M. (Eds.) *Magnetic Fabric: Methods*
414 *and Applications, Geol. Soc. Spec. Pub. 238*, London, pp. 49-59.
- 415 Jelinek, V., 1977. The statistical theory of measuring anisotropy of magnetic susceptibility of rocks
416 and its application. Geofyzika, Brno. 87pp

- 417 Jelinek, V., 1981. Characterization of the magnetic fabric of rocks. *Tectonophysics* 79, T63-T67.
- 418 Jelinek, V., 1996. Measuring anisotropy of magnetic susceptibility on a slowly spinning specimen –
419 basic theory. AGICO Print No 10, 27pp.
- 420 Kelso, P.R., Tikoff, B., Jackson, M., Sun, W., 2002. A new method for the separation of paramagnetic
421 and ferromagnetic susceptibility anisotropy using low field and high field methods. *Geophys.*
422 *J. Int.* 151, 345-359.
- 423 Kligfield, R., Owens W.H., Lowrie, W., 1981. Magnetic susceptibility anisotropy, strain, and
424 progressive deformation in Permian sediments from the Maritime Alps (France). *Earth Planet.*
425 *Sci. Lett.* 55, 181-189.
- 426 Nagata, T., 1961. *Rock Magnetism*, second ed., Maruzen, Tokyo.
- 427 Stacey, F.D., 1960. Magnetic anisotropy of igneous rocks. *J. Geophys. Res.* 65, 2429-2442.
- 428 Tarling, D.H., Hrouda, F., 1993. *The Magnetic Anisotropy of Rocks*. Chapman & Hall, London.